Observations of amplitude saturation in ELF/VLF wave generation by modulated HF heating of the auroral electrojet

R. C. Moore,[1] U. S. Inan,[1] and T. F. Bell[1]

Received 1 February 2006; revised 12 April 2006; accepted 25 May 2006; published 28 June 2006.

[1] We present detailed observations of the onset of amplitude saturation in ELF/VLF waves generated via modulated HF heating of naturally-forming, large-scale current systems, such as the auroral electrojet. Broadband ELF/VLF measurements at a ground-based receiver located near the High-Frequency Active Auroral Research Program (HAARP) HF transmitter in Gakona, Alaska, exhibit variations in signal amplitude which are qualitatively consistent with a hard-limiting approximation of the saturation process. A method to approximate the saturation curve as a function of HF power from experimental data is presented, and the results indicate that a ~5–10% reduction in generated ELF signal amplitude is typical at the maximum radiated HF power level (771 kW) for modulation frequencies between 1225 Hz and 3365 Hz. For HF transmissions using sinusoidal amplitude modulation, the saturation dominantly affects the second harmonic of the generated ELF/VLF signal, with amplitudes on average 16% lower than expected at the maximum HF power level. **Citation:** Moore, R. C., U. S. Inan, and T. F. Bell (2006), Observations of amplitude saturation in ELF/VLF wave generation by modulated HF heating of the auroral electrojet, *Geophys. Res. Lett.*, *33*, L12106, doi:10.1029/2006GL025934.

1. Introduction

[2] Modulated heating of the ionosphere in the presence of high-altitude, naturally-forming electric currents, such as the auroral electrojet and mid-latitude dynamo currents, has been investigated as a means for the generation of electromagnetic waves in the Extremely Low Frequency (ELF, 3-3000 Hz) and Very Low Frequency (VLF, 3–30 kHz) bands since the 1970s [*Getmantsev et al.*, 1974; *Stubbe et al.*, 1982; *Ferraro et al.*, 1984; *Barr and Stubbe*, 1991; *Inan et al.*, 2004]. Theoretical analyses of the HF absorption and the ELF/VLF wave generation process, such as those by *Tomko et al.* [1980] and *Papadopoulos et al.* [1990], indicate that an ionospheric conductivity saturation process may limit the efficiency of ELF/VLF wave production at high HF power levels. While the experimental results of *Ferraro et al.* [1984] and *Barr and Stubbe* [1991] show a nonlinear relationship between the generated ELF/VLF amplitude and the HF power, only the results of *Stubbe et al.* [1982] indicate that the variation may deviate from a log-linear relationship at high HF power levels.

[3] In this paper, we examine the characteristics of the generated ELF/VLF signals at the modulation frequencies and their harmonics as a function of radiated HF power. Our results show that a 0th-order (hard-limiting) approximation of the saturation mechanism qualitatively agrees with observations, and a method for the approximation of the saturation curve from experimental data is developed herein. Averages of the experimentally-derived saturation curves are presented, demonstrating the regular occurrence of saturation onset for HF transmissions at 3.25 MHz and at radiated HF power levels of 771 kW.

2. Instrumentation

[4] The data presented in this paper were acquired using an ELF/VLF receiver located in Chistochina, Alaska (~36 km from the HAARP facility at 62.61° N, 144.62° W). The receiver utilizes two orthogonal 4.8×4.8 m^2 air-core loop antennas oriented to detect the horizontal components of the wave magnetic field on the ground, a preamplifier located near the antennas, and a line-receiver and data recording system located ~600 meters from the antennas in order to reduce the effects of electromagnetic noise associated with 60 Hz hum and its harmonics. Both receiver channel inputs have RFI-suppression units to reduce interference from differential signals at frequencies above 100 kHz, including the HF band. The analog receiver channel outputs are anti-alias filtered at 40 kHz (using an 8-pole Chebyshev filter) and sampled at 100 kHz with 16-bit resolution. In post processing, the amplitude values associated with individual frequencies are extracted using a 10-Hz bandwidth FIR filter and decimated to 20 ms resolution. The amplitude values associated with each power step are extracted by taking the median value over the period of transmission in order to mitigate the effects of impulsive 'noise' signals, such as those introduced by lightning strokes in the form of radio atmospherics.

3. Description of the Experiment

[5] The experiment reported in this paper was conducted at the HAARP facility between July 30 and August 2, 2004, under both daytime and nighttime ionospheric conditions. Quiet geomagnetic conditions persisted throughout the majority of the campaign: the K_p index varied between 1 and 2^+ during transmission hours, and the absolute value of all components of the fluxgate magnetometer located in Gakona, AK, exceeded 50 nT during only three of the thirty-two hours of transmission. The HAARP HF transmitter broadcast at 3.25 MHz with X-mode polarization five twelve-second-long sinusoidal amplitude modulation periods at each of 1225, 1875, 2125, 2375, and 3365 Hz while stepping the modulated HF power linearly from 0 W to 771 kW (radiated power) in twelve one-second long steps. This

[1]Department of Electrical Engineering, Stanford University, Stanford, California, USA.

0094-8276/06/2006GL025934$05.00

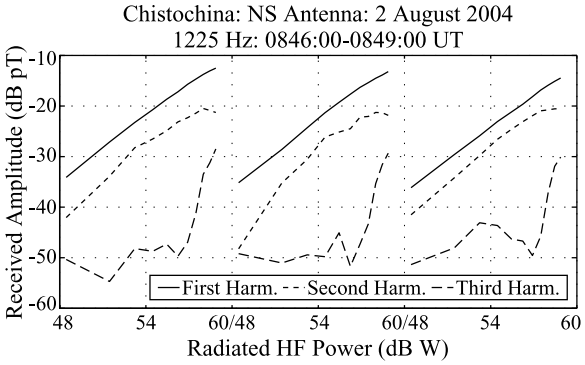

Figure 1. Amplitude of the first, second, and third harmonics observed during three successive power step transmissions on 2 August 2004.

sequence was repeated eight times per hour for eight hours per day. The HF beam was directed vertically for all transmissions. The input HF power at the HAARP facility (960 kW) is similar to the total power available for the Troms experiments (1.08 MW) [*Barr and Stubbe*, 1991]. The nonlinear characteristics associated with the transmission of a sinusoidally-modulated HF signal have been directly measured and accounted for in this analysis.

4. Experimental Data

[6] The 12-second-long power-step transmission pattern was repeated a total of 256 times for each modulation frequency over the four-day period of the experiment. Figure 1 shows the ELF/VLF signal amplitude at 1225 Hz and its second and third harmonics during three successive power-step periods with good (i.e., >10 dB) signal-to-noise ratio (SNR) at all three frequencies. The variation of amplitude with radiated power shown in Figure 1 holds throughout the data set when the signal amplitudes are observed to be above the noise floor: the amplitude of the fundamental component varies approximately log-linearly with radiated HF power; the amplitude of the second harmonic also appears to vary approximately log-linearly until it reaches a peak and subsequently begins to decrease with increasing radiated HF power; and the amplitude of the third harmonic rises above the noise when the amplitude of the second harmonic begins to significantly deviate from a log-linear variation. In all cases where the third harmonic amplitude is observed with SNR >10 dB, it emerges from the noise with a slope significantly larger than the first and second harmonics, as shown in Figure 1. However, the third harmonic was only observed with significant SNR for modulation frequencies of 1225 and 1875 Hz, due to the generally higher noise floors (primarily due to radio atmospherics) at the third harmonics of the higher modulation frequencies. It should be noted that our observations appear to be consistent with those of *Stubbe et al.* [1982], who showed a 0–50% power modulated waveform generated more ELF signal than a 50–100% power modulated waveform, despite having the same modulation depth.

[7] Although the amplitudes of the third harmonics seldom exhibit SNR levels >10 dB, the first and second harmonic amplitudes are observable at strong SNR levels on a regular basis. Figure 2 shows the campaign-averaged signal levels observed on the north-south antenna at Chistochina for each modulation frequency and its second harmonic. The second harmonic of the 3365 Hz tone is the only signal whose amplitude does not rise significantly (>10 dB) above the noise floor on average. Similar variations are observed on the East-West antenna. It is evident from Figure 2 that the variations observed under high SNR conditions shown in Figure 1 are generally representative of the variation of ELF/VLF amplitude with radiated HF power.

5. Analysis

[8] The log-linear relationship between the amplitude of the observed ELF/VLF signal, A_{ELF}, and the radiated HF power has been previously noted by *Papadopoulos et al.* [1990] and *Barr and Stubbe* [1991] and expressed as:

$$A_{\mathrm{ELF}} \propto A^{n-1}\left(\overline{P_{\mathrm{HF}}}\right)^{n} \tag{1}$$

where A is the area of the HF heated region, $\overline{P_{\mathrm{HF}}}$ is the transmitted HF power level, and n is an empirically determined power factor. In previous work, the value of n has been determined to vary between 0.5 and 1.1 [*Barr and Stubbe*, 1991, and references therein]. While the value of n may be greater than or less than 1, the term 'saturation' is used herein to describe only the circumstance when experimentally observed ELF/VLF amplitudes are less than that predicted by this log-linear variation.

[9] Equation (1) may be generalized in the following manner to account for a time-varying $P_{\mathrm{HF}}(t)$ and to provide the amplitudes of all frequencies of interest at the same time:

$$A_{\mathrm{ELF}}(\omega) = k(\omega)\left|\mathrm{DFT}\{(P_{\mathrm{HF}}(t))^{n}\}\right| \tag{2}$$

where $\mathrm{DFT}\{\cdot\}$ is the Discrete Fourier Transform operator and $k(\omega)$ is a factor that here incorporates the dependence of the ELF amplitude on the area of the heated ionospheric region and that is expected to vary with frequency due to the dependence of the ELF amplitude on such factors as the ionospheric heating and cooling time constants [*Papadopoulos et al.*, 2003].

[10] For the specific case of ideal sinusoidal amplitude modulation (100% depth) with a radiated HF power nor-

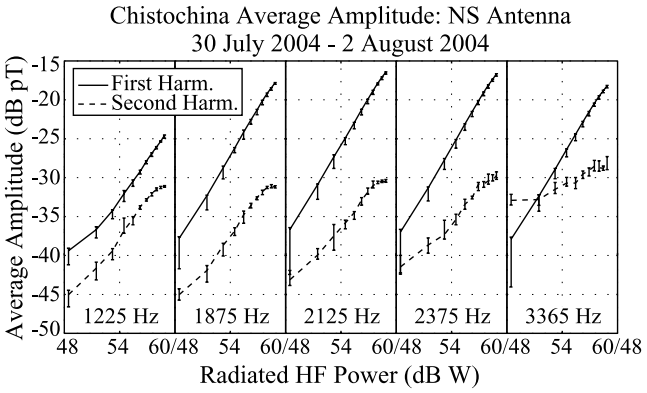

Figure 2. The campaign-averaged amplitude variations at each modulation frequency and second harmonic.

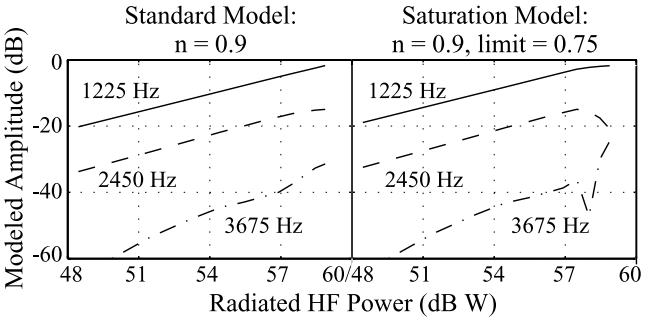

Figure 3. Modeled amplitude variation for the first, second, and third harmonics. (left) Saturation effects are omitted. (right) A hard-limiting saturation effect is included.

malized to 1 W, (2) may be re-expressed in the following manner:

$$A_{\mathrm{ELF}}(\omega) = k(\omega)\left|\mathrm{DFT}\left\{\left[\frac{3}{8}+\frac{1}{2}\cos\omega t+\frac{1}{8}\cos 2\omega t\right]^n\right\}\right| \qquad (3)$$

It can be seen from (3) that the second modulation frequency harmonic is present in the radiated HF power, equivalent, in this sense, to the role of the odd modulation frequency harmonics in the case of square-wave modulation. In our numerical analysis, we have also accounted for the nonlinearities associated with the HAARP HF transmission as well as the 95% depth of the modulation.

[11] The variations in amplitude that result from the application of (3) to the transmitted power-step sequence for $n = 0.9$ and $k(\omega) = 1$ are shown in Figure 3 (left). In this example, the nonlinearities present in the modulation envelope of the transmitted HF waveform are apparent in the deviation from strictly log-linear behavior. The variations in amplitude that result from employing a 0th-order (hard-limiting) saturation process to limit the HF power at 75% of the maximum value of $(P_{\mathrm{HF}}(t))^n$ are shown in Figure 3 (right). Comparing the experimental observations shown in Figure 1 with the strong deviation of the second harmonic from log-linear behavior and the abrupt increase in third harmonic amplitude at high HF power levels in Figure 3 leads to the conclusion that our simple model which accounts for a saturation process (i.e., deviation from the log-linear variation) produces results which qualitatively agree with observations.

[12] Although a 0th-order (hard-limiting) saturation process appears to qualitatively match the observations, it is unlikely that ionospheric HF absorption physically entails such hard-limiting saturation. In the remainder of this work, we approximate the saturation function based on experimental data. The expression for the ELF/VLF amplitude resulting from a given radiated HF power variation, incorporating the saturation model is:

$$A_{\mathrm{ELF}}(\omega) = k(\omega)|\mathrm{DFT}\{(P_{\mathrm{HF}}(t))^n f_{\mathrm{sat}}\{P_{\mathrm{HF}}(t)\}\}| \qquad (4)$$

where $f_{\mathrm{sat}}(\cdot)$ is the saturation function to be determined.

[13] In order to find an empirical form for $f_{\mathrm{sat}}(\cdot)$, we first determine the value of n which best fits the variation in amplitude of the first harmonic in a least-square-error sense. The comparison of the modeled first harmonic amplitudes shown in Figure 3 indicates that the first harmonic is largely unaffected by the saturation process until the last two power steps and thus provides our best measurement of n. By neglecting the amplitudes observed during the last two power steps, we may extract n from the observed variation of the amplitude of the first harmonic. Using this technique, 64% of the n's calculated throughout the campaign fell between .95 and 1.05. It should be noted that neglecting the amplitudes observed during the last two power steps produces higher values of n more than 95% of the time. With an approximation of n in hand, we then determine the saturation function, $f_{\mathrm{sat}}(\cdot)$. We assume that the slight deviation of the first harmonic amplitude from a log-linear dependence on HF power may be attributed to the saturation function:

$$f_{\mathrm{sat}}(k+1) = \left(\frac{A_{\mathrm{ELF}}(k+1)\overline{P_{\mathrm{HF}}(k)}^n}{A_{\mathrm{ELF}}(k)\overline{P_{\mathrm{HF}}(k+1)}^n}\right) f_{\mathrm{sat}}(k) \qquad (5)$$

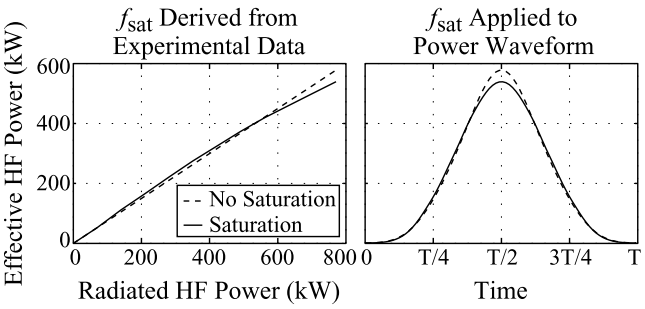

Figure 4. (left) The saturation function derived from experimental data and the variation expected from omitting saturation effects. (right) One period, T, of the instantaneous HF power waveform before and after the application of the saturation function.

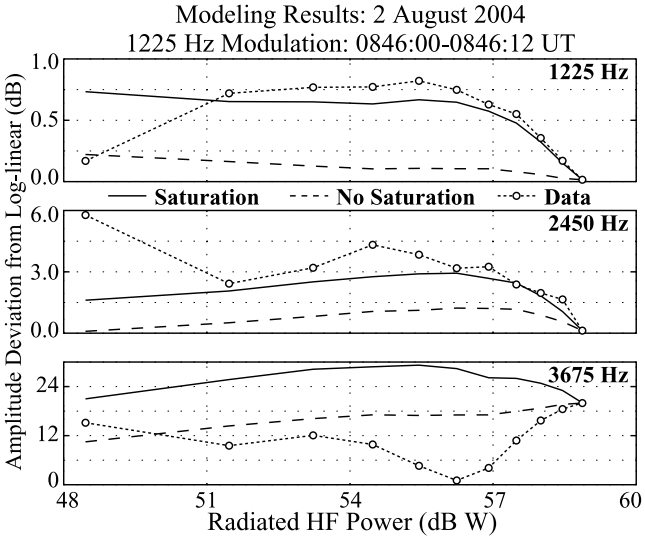

Figure 5. Comparison of the modeling results including and omitting saturation effects against the example data set. The calculated log-linear variation has been divided out of each trace in order to show the deviation from log-linearity.

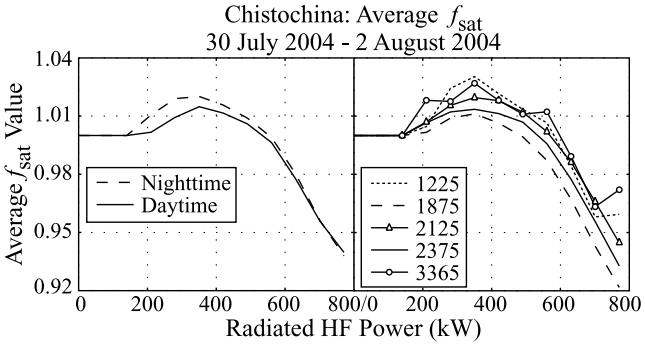

Figure 6. Average saturation functions. (left) Average daytime saturation versus average nighttime saturation. (right) A comparison of saturation as a function of modulation frequency.

where k is the index of the power step sequence. The values determined for f_{sat}, assuming that the first (lowest) HF power step does not yet lead to saturation (i.e., deviation from the log-linear variation), are then used to model the variation of the first, second, and third harmonic amplitudes using (4).

[14] For the first power-step series shown in Figure 1, the effective HF power, $(P_{HF}(t))^n f_{sat}\{P_{HF}(t)\}$, resulting from the analysis described above is shown in Figure 4 as a function of HF power and time. Although the values of the saturation function are allowed to take values above unity, they tend to values less than 1 at high radiated HF power levels, consistent with 'saturation', i.e., ELF/VLF values less than those predicted by the log-linear dependence.

[15] The resulting variation in amplitude at each frequency is then used to calculate the least-square-error values of $k(\omega)$. Figure 5 shows the modeled variation in amplitude for our example using both the method described by (3) and the method accounting for saturation described by (4). In Figure 5, the calculated log-linear variation with power has been divided out from each trace to allow for a more detailed inspection of the deviation from log-linearity. Although amplitude measurements of the second harmonic were not included in the determination of the saturation function, Figure 5 (middle) shows a $\sim$3 dB decrease in the modeled second harmonic amplitude at high HF power levels, closely matching observations. Figure 5 (bottom) shows that neither (3) nor (4) can account for the observed variation of the third harmonic amplitude. However, our model clearly captures the slight deviation from log-linear variation in the first harmonic amplitude along with the decrease in second harmonic amplitude at high radiated HF power levels.

[16] The campaign-averaged saturation functions extracted from the entire data set are shown in Figure 6 as a function of radiated HF power. Comparing the average daytime and average nighttime curves, the effects of saturation do not appear to depend on the time of day, indicating that the saturation process does not strongly depend on the ambient conductivity of the overlying ionosphere which varies significantly between nighttime and daytime. Figure 6 (right) shows that, on average, saturation effects reduce the total generated ELF/VLF signal level for all modulation frequencies by 5–10% at the highest radiated HF power level. Figure 6, together with the fact that the saturation model produces lower total errors than the standard log-linear model 93% of the time, indicates that saturation occurs at all modulation frequencies and under both daytime and nighttime conditions on a regular basis.

6. Discussion and Summary

[17] Experimental evidence of amplitude saturation in ELF/VLF waves produced by modulated HF heating of the auroral electrojet currents is presented. At the present maximum power level of HAARP and at a carrier frequency of 3.25 MHz with sinusoidal amplitude modulation, the saturation effect typically leads to a second harmonic amplitude which is 16% less than that expected with a log-linear dependence (of radiated ELF/VLF intensity on HF power) and a sharp 15 dB jump in the amplitude of the third harmonic. An empirical saturation function derived from measurements of the first harmonic amplitude produces results quantitatively consistent with amplitudes of the first and second harmonic frequencies. While a hard-cap saturation process qualitatively agrees with the variation of the third harmonic amplitude, this effect is not reproduced by the smoothly-varying saturation function. The regular occurrence of the observed saturation under both daytime and nighttime ionospheric conditions is demonstrated by the 5–10% reduction in value of the average saturation curves at high HF power levels. It thus appears that observations of ELF/VLF waves generated using the HAARP HF transmitter at full power and at 3.25 MHz may be interpreted as being generated in the saturation regime, in terms of the relationship of the HF absorption and corresponding ELF/VLF conductivity changes. Although the effects of saturation are observed readily using 3.25 MHz, the extent to which saturation occurs at other HF frequencies remains to be determined, due to the frequency-dependent nature of the ionospheric wave absorption process. The dependence of saturation on the modulation waveform also remains to be investigated. One experiment that may help further refine the saturation function calculation is to hold the average HF power constant while varying the depth of modulation. The planned upgrade of the HAARP facility in the near future should allow the investigation of this saturation process at higher HF power levels, perhaps allowing for a more detailed analysis of the third harmonic amplitude variation.

[18] **Acknowledgments.** This work was supported by the High-frequency Active Auroral Research Program (HAARP), the Defense Advanced Research Programs Agency (DARPA), and by the Office of Naval Research (ONR) via ONR grant N00014-03-0631 to Stanford University.

References

Barr, R., and P. Stubbe (1991), ELF radiation from the Troms "Super Heater" facility, *Geophys. Res. Lett.*, *18*, 1035–1038.

Ferraro, A. J., H. S. Lee, R. Allshouse, K. Carroll, R. Lunnen, and T. Collins (1984), Characteristics of ionospheric ELF radiation generated by HF heating, *J. Atmos. Sol. Terr. Phys.*, *46*, 855–865.

Getmantsev, C. G., N. A. Zuikov, D. S. Kotik, L. F. Mironenko, N. A. Mityakov, V. O. Rapoport, Y. A. Sazonov, V. Y. Trakhtengerts, and V. Y. Eidman (1974), Combination frequencies in the interaction between high-power short-wave radiation and ionospheric plasma, *JETP Lett.*, *20*, 101–102.

Inan, U. S., M. Golkowski, D. L. Carpenter, N. Reddell, R. C. Moore, T. F. Bell, E. Paschal, P. Kossey, E. Kennedy, and S. Z. Meth (2004), Multi-hop Whistler-mode ELF/VLF signals and triggered emissions excited by the HAARP HF heater, *Geophys. Res. Lett.*, *31*, L24805, doi:10.1029/2004GL021647.

Papadopoulos, K., C. L. Chang, P. Vitello, and A. Drobot (1990), On the efficiency of ionospheric ELF generation, *Radio Sci.*, *25*, 1311–1320.

Papadopoulos, K., T. Wallace, M. McCarrick, G. M. Milikh, and X. Yang (2003), On the efficiency of ELF/VLF generation using HF heating of the auroral electrojet, *Plasma Phys. Rep.*, *29*, 561–565.

Stubbe, P., H. Kopka, M. T. Rietveld, and R. L. Dowden (1982), ELF and VLF generation by modulated HF heating of the current carrying lower ionosphere, *J. Atmos. Sol. Terr. Phys.*, *44*, 1123–1135.

Tomko, A. A., A. J. Ferraro, and H. S. Lee (1980), *D* region absorption effects during high-power radio wave heating, *Radio Sci.*, *15*, 675–682.

T. F. Bell, U. S. Inan, and R. C. Moore, Department of Electrical Engineering, Stanford University, 350 Serra Mall, Stanford, CA 94305, USA. (bell@nova.stanford.edu; inan@nova.stanford.edu; berto@stanford.edu)